Inorganic Chemistry
Article

Inorg. Chem. **2011**, *50*, 317–324 **317**
DOI: 10.1021/ic1019873

Dye-Tethered Ruthenium Nitrosyls Containing Planar Dicarboxamide Tetradentate N4 Ligands: Effects of In-Plane Ligand Twist on NO Photolability

Nicole L. Fry, Brandon J. Heilman, and Pradip K. Mascharak*

Department of Chemistry and Biochemistry, University of California, Santa Cruz, California 95064, United States

Received September 28, 2010

To examine the steric effects of the in-plane ligands in dye-sensitized $\{RuNO\}^6$ nitrosyls on their NO photolability, two new ligands, namely, 1,2-Bis(pyridine-2-carboxamido)-4,5-dimethoxybenzene ($H_2(OMe)_2bpb$) and 1,2-Bis(Isoquinoline-1-carboxamido)-4,5-dimethoxybenzene ($H_2(OMe)_2IQ1$, H's are dissociable carboxamide protons) have been designed and synthesized. The syntheses and spectroscopic properties of $\{RuNO\}^6$ nitrosyls derived from these two ligands, namely, [((OMe)$_2$bpb)Ru(NO)(Cl)] (**4-Cl**), [((OMe)$_2$IQ1)Ru(NO)(Cl)] (**5-Cl**), [((OMe)$_2$bpb)Ru(NO)(Resf)] (**4-Resf**), and [((OMe)$_2$IQ1)Ru(NO)(Resf)] (**5-Resf**), are reported. The structures of **5-Cl**, **4-Resf**, and **5-Resf** have been determined by X-ray crystallography. Removal of the in-plane ligand twist in the quinoline-based R_2bQb^{2-} ligand frame (because of steric interactions between the extended quinoline ring systems) in both R_2bpb^{2-} and R_2IQ1^{2-} (pyridine and 1-isoquinoline rings, respectively, instead of quinoline rings in the equatorial plane) results in enhanced solution stability, as well as higher quantum yield values for NO photorelease upon exposure to 500 nm light. Both dye-tethered $\{RuNO\}^6$ nitrosyls **4-Resf** and **5-Resf** exhibit greater sensitivity to visible light compared to the chloro-bound species **4-Cl** and **5-Cl**. In addition, the dye-tethered nitrosyls are fluorescent and hence can be used as trackable NO donors in cellular studies.

Introduction

Nitric oxide (NO) plays an important role in many biological signaling processes including blood pressure regulation, neurotransmission, inflammatory response, and programmed cell death (apoptosis).[1−6] The regulatory role of NO in such processes has spurred the development of several exogenous NO donors as potential drugs.[7−9] For example, organic nitrites (RONO), nitrates ($RONO_2$), *S*-nitrosothiols (RSNO), and diazeniumdiolates (NONOates) have all been shown to deliver NO to cellular targets.[10,11] Recently, there has been increased interest in the deleterious role of NO and its ability to induce apoptosis in both healthy and malignant cells.[12,13] Development of site-specific NO donors could therefore be beneficial in selective killing of cancer cells.[14]

Phototriggered NO release from metal nitrosyls provides one such strategy for targeted delivery of NO to specific malignant sites. To this end, our group has synthesized several photoactive nitrosyls containing iron,[15] manganese,[16]

*To whom correspondence should be addressed. E-mail: pradip@chemistry.ucsc.edu.

(1) Ignarro, L. J. *Nitric Oxide: Biology and Pathobiology*; Academic Press: San Diego, 2000.
(2) *Nitric Oxide Free Radicals in Peripheral Neurotransmission*; Kalsner, S., Ed.; Birkhauser: Boston, 2000.
(3) Fukuto, J. M.; Wink, D. A. *Met. Ions Biol. Syst.* **1999**, *36*, 547–595.
(4) Ko, G. Y.; Fang, F. C. *Nitric Oxide and Infection*; Kluwer Academic/Plenum Publishers: New York, 1999.
(5) Lincoln, J.; Burnstock,G. *Nitric Oxide in Health and Disease*; Cambridge University Press: New York, 1997.
(6) *Nitric Oxide Research*; Feelisch, M., Stamler, J. S., Eds.; John Wiley and Sons: Chichester, U.K., 1996.
(7) Wang, P. G.; Cai, T. B.; Taniguchi, N. *Nitric Oxide Donors for Pharmaceutical and Biological Applications*; Wiley-VCH: Weinheim, Germany, 2005.
(8) (a) Degoute, C. S. *Drugs.* **2007**, *67*, 1053–1076. (b) Al-Sa'doni, H. H.; Ferro, A. *Rev. Med. Chem.* **2005**, *5*, 247–254. (c) Butler, A. R.; Megson, I. L. *Chem. Rev.* **2002**, *102*, 1155–1165.
(9) (a) Napoli, C.; Ignarro, L. J. *Annu. Rev. Pharmacol. Toxicol.* **2003**, *43*, 97–123. (b) Wang, P. G.; Xian, M.; Tang, X.; Wu, X.; Wen, X.; Cai, T.; Janczuk, A. J. *Chem. Rev.* **2002**, *102*, 1091–1134. (c) Wang, K.; Zhang, W.; Xian, M.; Hou, Y.-C.; Chen, X.-C.; Cheng, J.-P.; Wang, P. G. *Curr. Med. Chem.* **2000**, *7*, 821–834.
(10) (a) Keefer, L. K. *Curr. Top. Med. Chem.* **2005**, *5*, 625–636. (b) Hrabie, J. A.; Keefer, L. K. *Chem. Rev.* **2002**, *102*, 1135–1154.
(11) Wang, K.; Zhang, W.; Xian, M.; Hou, Y.-C.; Chen, X.-C.; Cheng, J.-P.; Wang, P. G. *Curr. Med. Chem.* **2000**, *7*, 821–834.
(12) (a) Mocellin, S.; Bronte, V.; Nitti, D. *Med. Res. Rev.* **2007**, *27*, 317–352. (b) Bobba, A.; Atlante, A.; Moro, L.; Calissano, P.; Marra, E. *Apoptosis* **2007**, *12*, 1597–1610. (c) Fukumura, D.; Kashiwagi, S.; Jain, R. K. *Nat. Rev. Cancer* **2006**, *6*, 521–534.
(13) (a) Hirst, D.; Robson, T. *J. Pharm. Pharmacol.* **2007**, *59*, 3–13. (b) Bonavida, B.; Khineche, S.; Huerta-Yepez, S.; Garban, H. *Drug Resist. Updates* **2006**, *9*, 157.
(14) (a) Eroy-Reveles, A. A.; Mascharak, P. K. *Future Med. Chem.* **2009**, *1* (8), 1497–1507. (b) Rose, M. J.; Mascharak, P. K. *Curr. Opin. Chem. Biol.* **2008**, *12*, 238–244. (c) Ford, P. C.; Bourassa, J.; Miranda, K.; Lee, B.; Lorkovic, I.; Boggs, S.; Kudo, S.; Laverman, L. *Coord. Chem. Rev.* **1998**, *171*, 185–202.
(15) (a) Afshar, R. K.; Patra, A. K.; Olmstead, M. M.; Mascharak, P. K. *Inorg. Chem.* **2004**, *43*, 5736–5743. (b) Patra, A. K.; Rowland, J. M.; Marlin, D. S.; Bill, E.; Olmstead, M. M.; Mascharak, P. K. *Inorg. Chem.* **2003**, *42*, 6812–6823. (c) Patra, A. K.; Afshar, R. K.; Olmstead, M. M.; Mascharak, P. K. *Angew. Chem., Int. Ed.* **2002**, *41*, 2512–2515.

Published on Web 11/29/2010

or ruthenium[17] metal centers. One benefit of ruthenium nitrosyls over those containing first row transition metals is their reduced reactivity toward oxygen and stability in water, both crucial for biological studies. However, these nitrosyls typically require ultraviolet (UV) light for photorelease of NO. To alleviate problems related to exposure of biological tissues to UV light, we have focused on sensitizing ruthenium nitrosyls to visible light.[18,19] A series $\{RuNO\}^6$ nitrosyls with various dicarboxamide tetradentate ligands, namely, [(Me_2bpb)-Ru(NO)(Cl)] (**1-Cl**), [(Me_2bQb)Ru(NO)(Cl)] (**2-Cl**), [(($OMe)_2$-bQb)Ru(NO)(Cl)] (**3-Cl**), have been successfully sensitized to 500 nm visible light via substitution of the chloride ligand with the conjugated dye resorufin (Resf).

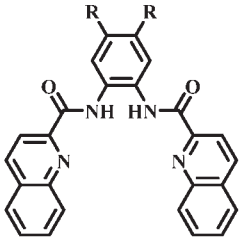

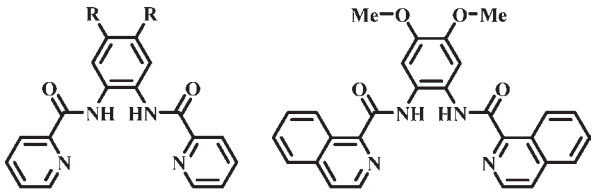

While the resulting resorufin-bound nitrosyls all exhibited absorption bands with λ_{max} of 500 nm, their efficiencies of NO photorelease upon exposure to 500 nm light can be modulated by rational substitutions in the in-plane ligand frame. For example, substitution of the pyridine donors in the ligand frame of [(Me_2bpb)Ru(NO)(Resf)] (**1-Resf**) with quinoline donors in [(Me_2bQb)Ru(NO)(Resf)] (**2-Resf**) and substitution of the methyl groups in (**2-Resf**) with more electron donating methoxy groups in [(($OMe)_2$bQb)Ru(NO)-(Resf)] (**3-Resf**) both result in higher quantum yield values at 500 nm ($\phi_{500} \approx 0.05$, 0.10, and 0.20, respectively).[18] The different ligand frames also lead to differences in the stabilities of the resorufin-bound nitrosyls in solution. For example, both quinoline containing **2-Resf** and **3-Resf** have reduced stability in aqueous solutions compared to **1-Resf** which comprises pyridine donors. Close examination of the structural features of these nitrosyls revealed that the ligand frames containing the quinoline donors (H_2R_2bQb) bind the $\{RuNO\}^6$ center in a twisted fashion because of steric interactions between the two quinoline moieties in the equatorial plane (Figure 1).[18] To probe the effect(s) of this twist on the stability and NO photolability of the resorufin-bound $\{RuNO\}^6$ nitrosyls, we have now designed two new dicarboxamide ligands containing methoxy-substituted phenylenediamine rings combined with pyridine ($H_2(OMe)_2$bpb) or 1-isoquinoline ($H_2(OMe)_2$IQ1) donors. Both new ligands bind the $\{RuNO\}^6$ center in a planar fashion (with no apparent twist, Figure 2) in the resulting chloride and resorufin-bound nitrosyls, namely, [(($OMe)_2$bpb)Ru(NO)(Cl)] (**4-Cl**), [(($OMe)_2$-IQ1)Ru(NO)(Cl)] (**5-Cl**), [(($OMe)_2$bpb)Ru(NO)(Resf)] (**4-Resf**), and [(($OMe)_2$IQ1)Ru(NO)(Resf)] (**5-Resf**). In this account, we report the syntheses and spectroscopic properties of **4-Cl**, **5-Cl**, **4-Resf**, and **5-Resf** in addition to the structures of **5-Cl**, **4-Resf**, and **5-Resf**. The stabilities of these nitrosyls in solutions and their NO-releasing capacities have also been examined critically to determine the effects of different substituents on the in-plane ligand frames and the resulting distortions arising from such substitutions. Much like **1-Resf**, **2-Resf**, and **3-Resf**, the present set of nitrosyls exhibit strong fluorescence and adds to the repertoire of "trackable NO donors".[18b]

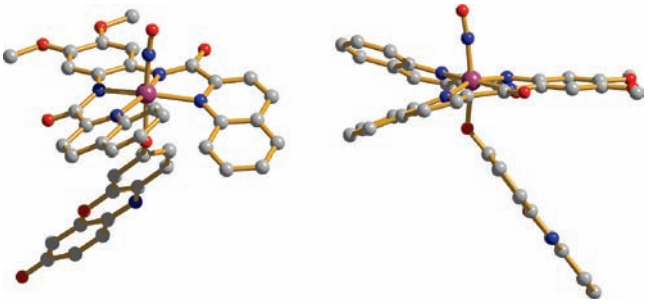

Figure 1. X-ray structure of [(($OMe)_2$bQb)Ru(NO)(Resf)] from front angle (left) and side angle (right) displaying twist of the in plane tetradentate ligand. H atoms are omitted for the sake of clarity.

Figure 2. Design of the new ligand $(OMe)_2$IQ1, intended for relieving twist in the equatorial plane of the Resf-tethered $\{RuNO\}^6$ nitrosyls.

Experimental Section

Materials. NO gas was purchased from Spectra Gases Inc. and was purified by passing through a long KOH column prior to use. $RuCl_3 \cdot xH_2O$ (Aldrich Chemical Co.) was treated several times with concentrated HCl to prepare the starting metal salt, $RuCl_3 \cdot 3H_2O$. The solvents were dried by standard techniques and distilled. 1-Isoquinoline was purchased from Wako Chemicals. 1,2-Dimethoxy-4,5-diaminobenzene was synthesized according to

(16) (a) Hoffman-Luca, G. C.; Eroy-Reveles, A. A.; Alvarenga, J.; Mascharak, P. K. *Inorg. Chem.* **2009**, *48*, 9104–9111. (b) Eroy-Reveles, A. A.; Leung, Y.; Beavers, C. M.; Olmstead, M. M.; Mascharak, P. K. *J. Am. Chem. Soc.* **2008**, *130*, 4447–4458. (c) Eroy-Reveles, A. A.; Leung, Y.; Mascharak, P. K. *J. Am. Chem. Soc.* **2006**, *128*, 7166–7167.

(17) (a) Fry, N. L.; Rose, M. J.; Rogow, D. L.; Nyitray, C.; Kaur, M.; Mascharak, P. K. *Inorg. Chem.* **2010**, *49*, 1487–1495. (b) Rose, M. J.; Mascharak, P. K. *Coord. Chem. Rev.* **2008**, *252*, 2093–2114. (c) Rose, M. J.; Patra, A. K.; Alcid, E. A.; Olmstead, M. M.; Mascharak, P. K. *Inorg. Chem.* **2007**, *46*, 2328–2338. (d) Patra, A. K.; Rose, M. J.; Murphy, K. A.; Olmstead, M. M.; Mascharak, P. K. *Inorg. Chem.* **2004**, *46*, 4487–4495.

(18) (a) Rose, M. J.; Olmstead, M. M.; Mascharak, P. K. *J. Am. Chem. Soc.* **2007**, *129*, 5342–5343. (b) Rose, M. J.; Fry, N. L.; Marlow, R.; Hinck, L.; Mascharak, P. K. *J. Am. Chem. Soc.* **2008**, *130*, 8834–8846.

(19) Rose, M. J.; Mascharak, P. K. *Inorg. Chem.* **2009**, *48*, 6904–6917.

the published procedure.[20] All other chemicals were purchased from Aldrich Chemical Co. and used without further purification.

Synthesis of Ligands. 1,2-Bis(pyridine-2-carboxamido)-4,5-dimethoxybenzene ($H_2(OMe)_2$bpb, H's Are Dissociable Carboxamide Protons). A mixture of 1,2-dimethoxy-4,5-diaminobenzene (0.51 g, 3.0 mmol), 2 equiv of picolinic acid (0.74 g, 6.0 mmol), and 2 equiv of $P(OPh)_3$ (1.87 g, 6.0 mmol) was dissolved in 20 mL of pyridine. The resulting green/brown solution turned amber after refluxing for 4 h. The solution was cooled and kept at 4 °C overnight. The resulting tan precipitate was filtered and washed with EtOH and Et_2O and dried in vacuo. Yield: 1.04 g (55%). Selected IR bands (KBr disk, in cm^{-1}): 3335 (w, ν_{NH}), 3285 (w), 1676 (s $\nu_{C=O}$), 1662 (s), 1609 (w), 1527 (s), 1504 (s), 1480 (m), 1350 (m), 1210 (vs), 1093 (m), 997 (m), 751 (m), 671 (m). ^{1}H NMR in $CDCl_3$, δ from TMS: 10.32 (s 2H), 8.57 (d 2H), 8.32 (d 2H), 7.91 (t 2H), 7.47 (m 4H), 3.94 (s 6H).

1,2-Bis(Isoquinoline-1-carboxamido)-4,5-dimethoxybenzene ($H_2(OMe)_2$IQ1, H's Are Dissociable Carboxamide Protons). A solution containing 1 equiv of 1,2-dimethoxy-4,5-diaminobenzene (1.27 g, 7.56 mmol), 2 equiv of 1-Isoquinolinecarboxylic acid (2.62 g, 15.1 mmol), and 2 equiv of $P(OPh)_3$ (4.69 g, 15.10 mmol) was prepared in 40 mL of pyridine. The green solution turned bright red upon heating at 100 °C for 4 h. The solution was partially condensed and stored at 4 °C overnight. The resulting bright yellow-orange precipitate was filtered and washed several times with EtOH and Et_2O and dried in vacuo. Yield: 2.17 g (60%). Selected IR frequencies (KBr disk, in cm^{-1}): 3296 (w, ν_{NH}), 1682 (s, $\nu_{C=O}$), 1526 (vs), 1478 (s), 1334 (w), 1205 (s), 1108 (w). ^{1}H NMR in $CDCl_3$, δ from TMS: 10.46 (s 2H), 9.72 (d 2H), 8.40 (d 2H), 7.88 (d 2H), 7.82 (d 2H), 7.73 (t 4H), 7.53 (s H).

Syntheses of Metal Complexes. [($(OMe)_2$bpb)Ru(NO)(Cl)] (4-Cl). A pale yellow solution of $H_2(OMe)_2$bpb (0.20 g, 0.53 mmol) in 20 mL of *N,N*-dimethylformamide (DMF) was treated with 2.1 equiv of NaH (0.03 g, 1.10 mmol) to generate a bright orange solution. A batch of 0.14 g (0.53 mmol) of $RuCl_3 \cdot 3H_2O$ was then added to the solution of deprotonated ligand, and the green mixture was heated to reflux temperature for 16 h. Next, it was cooled to room temperature and filtered to remove solid NaCl. The dark green filtrate was degassed and NO gas was bubbled through the solution at reflux temperature for 1 h. The resulting red/orange solution was cooled, and the solvent was removed in vacuo. The oily residue was triturated several times with MeCN to remove DMF. The solid was finally washed with portions of MeCN (2 × 5 mL) and tetrahydrofuran (THF, 2 × 5 mL) to afford an orange-brown compound which was dried in vacuo. Yield: 0.21 g (72%). Anal. Calcd. for $C_{20}H_{16}ClN_5O_5Ru$: C 44.28, H 2.95, N 12.92; Found: C 44.53, H 3.01, N 12.89. Selected IR bands (KBr disk, in cm^{-1}): 1845 (vs, ν_{NO}), 1631 (vs, $\nu_{C=O}$), 1596 (m), 1566 (w), 1497 (s), 1402 (m), 1368 (m), 1278 (w), 1254 (m), 1080 (w), 988 (w), 872 (w), 756 (w), 489 (w). UV/vis in DMF, λ in nm (ε in M^{-1} cm^{-1}): 319 (12 500), 420 (7 800). ^{1}H NMR in CDCl3, δ from TMS: 8.74 (d 2H), 8.49 (s 2H), 8.39 (d 2H), 8.24 (t 2H), 7.74 (t 2H), 3.98 (s 6H).

[($(OMe)_2$bpb)Ru(NO)(Resf)] (4-Resf). A mixture of [($(OMe)_2$bpb)Ru(NO)(Cl)] (0.10 g, 0.18 mmol) and 1 equiv of $AgBF_4$ (0.04 g, 0.18 mmol) in 30 mL of MeCN was heated to reflux for 15 min and then a batch of 0.04 g (0.18 mmol) of Resorufin (sodium salt) was added. The resulting red solution was heated to reflux for an additional 16 h. The red/orange mixture thus obtained was filtered and concentrated under vacuum and then stored at 4 °C for 12 h. The red precipitate thus obtained was filtered and washed with ether (2 × 5 mL). Yield: 0.04 mg (27%). Anal. Calcd. for $C_{32}H_{22}N_6O_8Ru$: C 53.41, H 3.06, N 11.68; Found: C 53.37, H 3.12, N 11.89. Selected IR bands (KBr disk, in cm^{-1}): 1831 (s, ν_{NO}), 1630 (vs, $\nu_{C=O}$), 1592 (vs), 1485 (vs), 1403 (m), 1370 (m), 1322 (w), 1272 (s), 1205 (m), 1102 (m), 1082 (m), 863 (m), 758(w), 683 (w), 588 (w), 493 (m). UV/vis in MeCN, λ in nm (ε in M^{-1} cm^{-1}): 402 (14 600), 495 (29 000). ^{1}H NMR in $CDCl_3$, δ from TMS: 8.75 (d 2H), 8.52 (d 2H), 8.32 (s 2H), 8.13 (t 2H), 7.81 (t 2H), 7.56 (t 2H), 7.30 (d 1H), 7.12 (2 1H), 6.72 (d 1H), 6.11 (s 1H), 6.08 (d 1H), 5.67 (s 1H), 4.00 (s 6H).

[($(OMe)_2$IQ1)Ru(NO)(Cl)] (5-Cl). A yellow solution of $H_2(OMe)_2$IQ1 (0.15 g, 0.31 mmol) in 20 mL of DMF was treated with 2.1 equiv of NaH (0.02 g, 0.67 mmol) to generate a red solution and to it was added a batch of 0.08 g (0.31 mmol) of $RuCl_3 \cdot 3H_2O$. The dark brown mixture was then heated to reflux temperature for 20 h. Next, the green-brown solution was cooled to room temperature and filtered to remove NaCl. The filtrate was degassed, and NO gas was bubbled through it at reflux temperature for 2 h. The resulting red/maroon solution was cooled, and the solvent was removed in vacuo. The oily residue was triturated several times with MeCN to afford a red-brown solid. This solid was then stirred in hot MeCN and filtered to remove impurities. The dark maroon solid was finally washed with Et_2O and dried in vacuo. Yield: 0.16 g (80%). Anal. Calcd. for $C_{28}H_{20}ClN_5O_5Ru$: C 52.34, H 3.12, N 10.90; Found: C 52.12, H 3.22, N 10.53. Selected IR frequencies (KBr disk, in cm^{-1}): 2923 (w), 1832 (m ν_{NO}), 1614 (vs), 1585 (s), 1492 (s), 1253 (s), 1091 (s). ^{1}H NMR in $CDCl_3$, δ from TMS: 10.45 (d 2H), 8.72 (d 2H), 8.61 (s H), 8.06 (d 2H), 7.90 (d 2H), 7.93 (t 2H), 7.90 (t 2H), 4.05 (s 6H). UV/vis in DMF, λ in nm (ε in M^{-1} cm^{-1}): 290 (27 000), 320 sh (22 300), 475 (8 700).

[($(OMe)_2$IQ1)Ru(NO)(Resf)] (5-Resf). A solution of [($(OMe)_2$IQ1)Ru(NO)(Cl)] (0.13 g, 0.20 mmol) in 20 mL of MeCN was treated with $AgBF_4$ (0.04 g, 0.20 mmol) and heated to reflux temperature for 3 h. Next, a batch of 0.05 g (0.20 mmol) of Resorufin dye (as Na salt) was added to the hot maroon solution and continued to reflux for 4 h. The resulting bright red solution was cooled to 4 °C, and the dark red precipitate was filtered. The dried precipitate was then redissolved in CH_2Cl_2 and filtered to remove AgCl and $NaBF_4$. The filtrate was concentrated and loaded on a silica gel column. A CH_2Cl_2/THF gradient was used to elute the final product (40% THF). Yield: 0.08 g (45%). Anal. Calcd. for $C_{40}H_{26}N_6O_8Ru$: C 58.61, H 3.17, N 10.26; Found: C 58.45, H 3.31, N 10.37. Selected IR frequencies (KBr disk, in cm^{-1}): 1827 (vs ν_{NO}), 1617 (s), 1580 (m), 1487 (s), 1323 (m), 1270 (s), 1266 (s), 1199 (m), 1095 (m), 849 (w), 491 (w) . ^{1}H NMR in $CDCl_3$, δ from TMS: 10.27 (d 2H), 8.78 (d 2H), 8.55 (s 2H), 8.14 (d 2H), 8.01 (d 2H), 7.92 (t 2H), 7.83 (t 2H), 7.24 (s 1H), 7.03 (d 1H), 6.72 (d 1H), 5.99 (s 1H), 5.97(d 1H), 5.36 (d 1H), 4.09 (s 6H). UV/vis in MeCN, λ in nm (ε in M^{-1} cm^{-1}): 330 (15 000), 495 (30 000).

Physical Measurements. The ^{1}H NMR spectra were recorded at 298 K on a Varian Inova 500 MHz instrument. A Perkin-Elmer Spectrum-One FT-IR spectrometer was used to monitor the IR spectra of the complexes. The electronic absorption spectra were obtained with a scanning Cary 50 spectrophotometer (Varian Associates). Fluorescence spectra were recorded with a Perkin-Elmer LS50B Fluorescence/Luminescence Spectrometer. Release of NO in aqueous solution upon illumination was monitored by using the *in*NO Nitric Oxide Monitoring System (Innovative Instruments, Inc.) fitted with the *ami*-NO 2008 electrode. The NO amperograms were recorded using stirred solutions contained in open vials.

X-ray Crystallography. Vapor diffusion of diethyl ether into a solution of **4-Resf** in $CHCl_3$ at 4 °C afforded red crystalline blades suitable for X-ray studies. Red crystals of **5-Cl**, suitable for diffraction study, were obtained via vapor diffusion of pentane into a solution of **5-Cl** in $CHCl_3$ at room temperature. Vapor diffusion of diethyl ether into a CH_2Cl_2/THF solution of **5-Resf** at room temperature afforded red crystals used for the structural studies. Diffraction data for **4-Resf**·$2CHCl_3 \cdot (0.5)Et_2O$, **5-Cl**·$2CHCl_3$, and **5-Resf** were collected at 150 K on a Bruker APEX-II instrument using monochromated Mo−Kα radiation (λ = 0.71073 Å). All diffraction data were corrected for absorption, and calculations were performed using the SHELXTL

(20) Rosa, D. T.; Reynolds, R. A.; Malinak, S. M.; Coucouvanis, D. *Inorg. Synth.* **2002**, *33*, 112–119.

Table 1. Summary of Crystal Data, Intensity Collection and Refinement Parameters for $[((OMe)_2bpb)Ru(NO)(Resf)]\cdot(CHCl_3)_2(OEt_2)_{0.5}$ (**4-Resf**·$2CHCl_3\cdot(0.5)Et_2O$), $[((OMe)_2IQ1)Ru(NO)(Cl)]\cdot(CHCl_3)_2$ (**5-Cl**·$2CHCl_3$), $[((OMe)_2IQ1)Ru(NO)(Resf)]$ (**5-Resf**)

	4-Resf	**5-Cl**	**5-Resf**
empirical formula	$C_{36}H_{29}Cl_6N_6O_{8.5}Ru$	$C_{30}H_{22}Cl_7N_5O_5Ru$	$C_{40}H_{26}N_6O_8Ru$
formula weight	995.42	881.75	819.74
crystal color	red blades	red blades	red blades
crystal size (mm^3)	0.12 × 0.08 × 0.07	0.11 × 0.02 × 0.02	0.090 × 0.050 × 0.010
temperature (K)	150(2)	150(2)	150(2)
wavelength (Å)	0.71073	0.71073	0.71073
crystal system	triclinic	monoclinic	triclinic
space group	$P\bar{1}$	$P2_1/c$	$P\bar{1}$
a (Å)	11.1266(11)	12.2656(11)	8.765(10)
b (Å)	12.1021(12)	16.9131(15)	11.534(13)
c (Å)	15.7732(16)	20.0497(13)	16.827(18)
α (deg)	74.0320(10)	90	94.414(12)
β (deg)	77.7320(10)	127.317(4)	91.102(11)
γ (deg)	85.4830(10)	90	97.487(12)
V ($Å^3$)	1994.9(3)	3307.9(5)	1681(3)
Z	2	4	2
d_{cal} (g/cm^3)	1.657	1.771	1.620
μ (mm^{-1})	0.856	1.089	0.535
GOF[a] on F^2	1.033	1.012	1.025
final R indices	R_1 = 0.0454	R_1 = 0.0343	R_1 = 0.0392
[$I > 2\sigma(I)$]	wR_2 = 0.1042	wR_2 = 0.0691	wR_2 = 0.0806
R indices[b]	R_1 = 0.0570	R_1 = 0.0559	R_1 = 0.0552
All data[c]	wR_2 = 0.1114	wR_2 = 0.0769	wR_2 = 0.0865

[a] GOF = $[\sum w(F_o^2 - F_c^2)^2/(N_o - N_v)]^{1/2}$ (N_o = number of observations, N_v = number of variables). [b] $R_1 = \sum||F_o| - |F_c||/\sum|F_o|$. [c] $wR_2 = [\sum w(F_o^2 - F_c^2)^2/\sum w|F_o|^2)]^{1/2}$.

Table 2. Selected Bond Distances (Å) and Angles (deg) of **4-Resf**, **5-Cl** and **5-Resf**

	4-Resf	**5-Cl**	**5-Resf**
	Bond Distances		
Ru−N5	1.729(4)	1.735(3)	1.732(3)
N5−O5	1.169(4)	1.153(3)	1.167(3)
Ru−N1	2.131(3)	2.132(3)	2.115(3)
Ru−N2	1.982(3)	1.984(3)	1.975(3)
Ru−N3	1.980(3)	1.970(3)	1.977(3)
Ru−N4	2.133(3)	2.105(3)	2.128(3)
Ru−Cl1		2.361(1)	
Ru−O6	2.004(3)		2.022(2)
	Bond Angles		
Ru−N5−O5	169.3(3)	175.9(2)	176.5(3)
N5−Ru− Cl1		174.8(1)	
N5−Ru− O6	172.5(1)		170.7(1)

(1995−99) software package (Bruker Analytical X-ray Systems Inc.) for structure solution and refinement. Additional refinement details are contained in the CIF files (Supporting Information). Instrument parameters, crystal data, and data collection parameters for all the complexes are summarized in Table 1. Selected bond distances and bond angles for **4- Resf**·$2CHCl_3\cdot(0.5)Et_2O$, **5-Cl**·$2CHCl_3$, and **5-Resf** are listed in Table 2.

Photolysis Experiments. The quantum yield (ϕ) values were obtained using a tunable Apex Illuminator (150W xenon lamp) equipped with a Cornerstone 130 1/8 M monochromator (measured intensity of ~10 mW). Actinochrome N (475/610) was used to determine the quantum yield values at 500 nm (ϕ_{500}). Solutions of **4-Cl**, **4-Resf**, **5-Cl**, and **5-Resf** were prepared and placed in 2 × 10 mm quartz cuvettes, 1 cm away from the light source. All solutions were prepared to ensure sufficient absorbance (>90%) at the irradiation wavelength, and changes in electronic spectrum at 788, 650, 630, and 660 nm for **4-Cl**, **4-Resf**, **5-Cl**, and **5-Resf**, respectively (<10% photolysis), were used to determine the extent of photorelease of NO.

Results and Discussion

To remove the twist of the bQb^{2-} ligand frame in the equatorial planes of **2-Cl**, **2-Resf**, **3-Cl**, and **3-Resf**, we included the more spread-out 1-isoquinoline groups in the designed ligand $H_2(OMe)_2IQ1$ in the present work. Such a change did not affect the extended conjugation in the ligand frame. Since the methoxy groups were retained, the electron donating ability of the $H_2(OMe)_2IQ1$ ligand was hardly altered. The overall design therefore ensured removal of the twist in the coordinated ligand in the equatorial plane of the nitrosyls with minimum changes in other parameters (Figure 2). To complete the investigation on the effect(s) of the twist, we also designed the methoxy substituted pyridine-based ligand, $H_2(OMe)_2bpb$. When coordinated, the pyridine rings of this ligand remain far apart in the equatorial plane of the nitrosyls and hence no steric interaction between them is expected (Figure 2).

Reaction of $RuCl_3$ with the deprotonated (with NaH) ligands in DMF followed by the addition of NO(g) produces the chloride bond species $[((OMe)_2bpb)Ru(NO)(Cl)]$ (**4-Cl**) and $[((OMe)_2IQ1)Ru(NO)(Cl)]$ (**5-Cl**). Further reaction of these chloro complexes with $AgBF_4$ in MeCN results in the formation of the MeCN-bound intermediates which afford **4-Resf** and **5-Resf** upon reaction with the sodium salt of the resorufin dye. In the final products, either a Cl^- or a $Resf^-$ ligand is bound trans to NO.

All four nitrosyls are soluble in solvents like $CHCl_3$, MeCN, DMF, and dimethylsulfoxide (DMSO). When dissolved in weakly coordinating aprotic solvents like $CHCl_3$ and MeCN, the nitrosyls are indefinitely stable and do not lose the bound resorufin dye. However, in solvents like DMSO or in aqueous solutions (pH 5−7), the resorufin-bound nitrosyls slowly lose the bound dye over the course of several hours. Compared to the $\{RuNO\}^6$ nitrosyls containing twisted quinoline ligands, namely, **2-Resf** and **3-Resf**, which lose ~20% bound dye in 1 h, **5-Resf** loses ~10% bound dye within the same time. The two pyridine-containing nitrosyls **1-Resf** and **4-Resf** both lose less than 5% bound dye in 1 h. The dye bound nitrosyls derived from planar ligand frames with no twist thus exhibit increased stability in H_2O. While

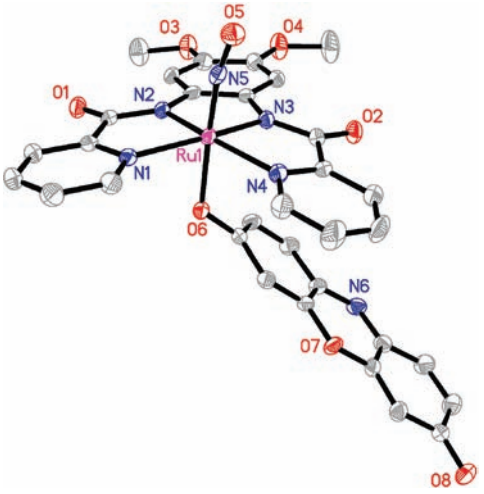

Figure 3. Thermal ellipsoid (probability level 50%) plot of [((OMe)$_2$bpb)-Ru(NO)(Resf)] (**4-Resf**) with select atom-labeling. H atoms are omitted for the sake of clarity.

the stability of **5-Resf** is improved compared to that of the {RuNO}^{6} nitrosyls with twisted quinoline ligand frames, **5-Resf** is still slightly less stable than the pyridine-containing nitrosyls **1-Resf** and **4-Resf**. Collectively, the results suggest that the use of planar pyridine-based ligand frames provides the most stability in these designed dye-tethered {RuNO}^{6} nitrosyls.

Structure of the Complexes. [((OMe)$_2$bpb)Ru(NO)(Resf)] (4-Resf). The tetradentate (OMe)$_2$bpb^{2-} ligand frame of **4-Resf** is bound to the ruthenium center in a planar fashion occupying the equatorial plane (Figure 3). The pseudo-octahedral structure is completed with the phenolato-O bound resorufin dye trans to NO at the axial positions. The Ru−N5−O5 bond angle is slightly bent at 169.3(3)° (Table 2). The substitution of methoxy groups in **4-Resf** compared to methyl groups in **1-Resf** does little to alter the overall geometry of the two structures. In both cases, the resorufin dye is tilted away from the equatorial plane with ∼120 ° Ru−O6−C(Resf) bond angles (**1-Resf** = 128.46(11)°,[18b] **4-Resf** = 126.0(3)°) implying that the bound oxygen is more sp^2 than sp^3 hybridized. The dye is positioned in such a way that it is directly below one of the pyridine rings of the equatorial ligand and presumably provides favorable $\pi-\pi$ interactions that stabilize the structures of both **1-Resf** and **4-Resf**. As a result, this pyridine ring is very slightly off the plane of the rest of the ligand frame. The Ru−N5 (1.729(4) Å) and N5−O5 (1.169(4) Å) bonds lengths of **4-Resf** are also similar to those of **1-Resf** (1.7347(16)[18b] and 1.159(2) Å respectively).

[((OMe)$_2$IQ1)Ru(NO)(Cl)] (5-Cl). The presence of 1-isoquinoline moieties in the tetradentate (OMe)$_2$IQ1^{2-} ligand instead of regular quinoline (as in (OMe)$_2$bQb^{2-}) allows the ligand to remain *strictly planar* when bound to the ruthenium center in the equatorial plane of **5-Cl** (Figure 4). This is in contrast to the steric interaction of the extended quinoline groups in the (OMe)$_2$bQb^{2-} ligand of **3-Cl** that led to the twisting of the ligand (∼35°) as noted in our previous work (Figure 5).[19] A chloride ligand is bound trans to NO in the axial positions generating a nearly octahedral geometry in the structure of **5-Cl**. Examination of bond lengths in Table 2 reveals that the Ru−N5(O) (1.735(3) Å) and N5−O5 (1.153(3) Å) bond lengths

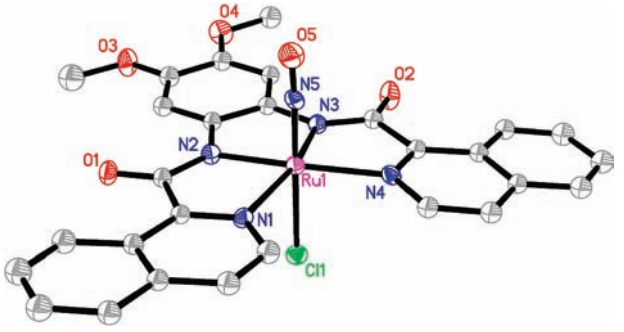

Figure 4. Thermal ellipsoid (probability level 50%) plot of [((OMe)$_2$-IQ1)Ru(NO)(Cl)] (**5-Cl**) with select atom-labeling. H atoms are omitted for the sake of clarity.

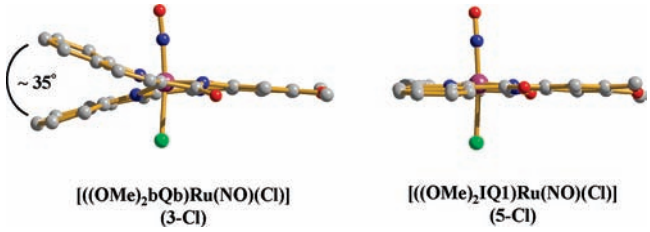

Figure 5. X-ray structure of [((OMe)$_2$bQb)Ru(NO)(Cl)] (left) and [((OMe)$_2$IQ1)Ru(NO)(Cl)] (right) displaying twist of the in-plane tetradentate ligand. H atoms are omitted for the sake of clarity.

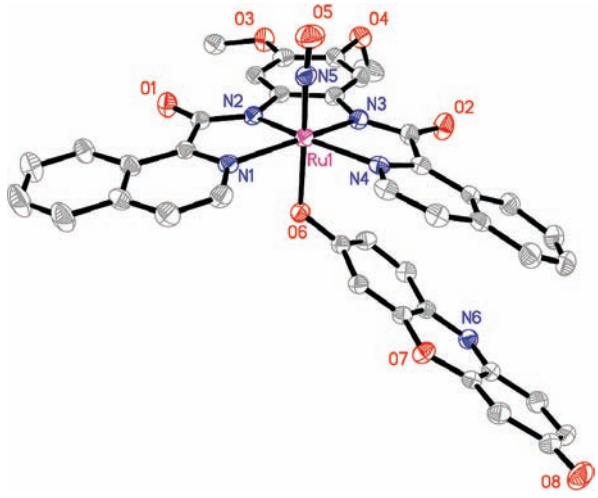

Figure 6. Thermal ellipsoid (probability level 50%) plot of [((OMe)$_2$-IQ1)Ru(NO)(Resf)] (**5-Resf**) with selected atom-labeling. H atoms are omitted for the sake of clarity.

of **5-Cl** are very similar to those of **3-Cl** (1.7457(18) and 1.148(2) Å[19] respectively). Both nitrosyls contain almost linear Ru−N5−O5 bond angles (**3-Cl** = 175.73(19) Å;[19] **5-Cl** = 175.9(2) Å), typical of {RuNO}^{6} nitrosyls.

[((OMe)$_2$IQ1)Ru(NO)(Resf)] (5-Resf). The (OMe)$_2$IQ1^{2-} ligand frame of **5-Resf** is bound to the ruthenium center in the equatorial plane while the resorufin dye is trans to NO at the axial positions (Figure 6). Here also, the resorufin dye is bound through the phenolato-O and a similar tilt of the bound dye (Ru−O6−C(Resf) angle of 126.3(2)°) is observed. The position of the bound resorufin is such that the rings of the dye are aligned parallel to the rings of one of the 1-isoquinoline moieties in the (OMe)$_2$IQ1^{2-} ligand frame of **5-Resf**. This $\pi-\pi$ interaction causes the 1-isoquinoline moiety of (OMe)$_2$IQ1^{2-} to tilt *slightly* out of the plane of the rest of

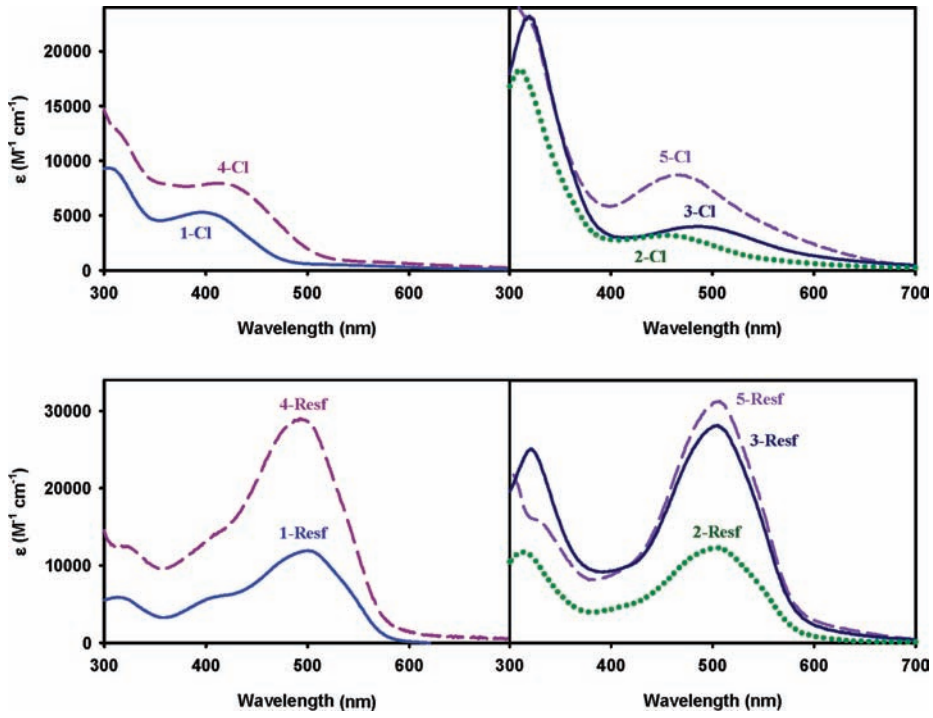

Figure 7. Electronic absorption spectra of **1-Cl**[17d] and **4-Cl** (top left), **2-Cl**,[17d] **3-Cl**,[19] and **5-Cl** (top right) in DMF. Electronic absorption spectra of **1-Resf**[18b] and **4-Resf** (bottom left), and **2-Resf**,[18b] **3-Resf**,[18b] and **4-Resf** (bottom right) in $CHCl_3$.

the tetradentate ligand frame. Despite this tilt of the ligand in the equatorial plane, **5-Resf** is significantly more planar than that of **3-Resf** which contains the regular quinoline ligand, $(OMe)_2bQb^{2-}$. The Ru-NO unit in **5-Resf** comprises Ru−N5(O) and N5−O5 bond lengths of 1.732(3) Å and 1.167(3) Å, respectively, which fall within the ranges observed in the other resorufin nitrosyls (1.729 −1.7425 Å and 1.154−1.169 Å, respectively).[18b] In addition, the Ru−N5−O5 bond angle of **5-Resf** is almost linear (176.5(3)°) as expected for a $\{RuNO\}^6$ nitrosyl.

Spectroscopic Properties. The carbonyl stretching frequency ($\nu_{C=O}$) of the free ligand $H_2(OMe)_2bpb$ (1676 cm^{-1}) shifts to lower energy upon formation of complexes **4-Cl** (1631 cm^{-1}) and **4-Resf** (1630 cm-1) (Supporting Information, Figure S1−S2). Similar lowering of $\nu_{C=O}$ value of $H_2(OMe)_2IQ1$ (1682 cm^{-1}) is observed in **5-Cl** (1614 cm^{-1}) and **5-Resf** (1617 cm^{-1}) (Supporting Information, Figure S3−S4). The NO stretching frequencies (ν_{NO}) of **4-Cl** (1845 cm^{-1}), **4-Resf** (1831 cm^{-1}), **5-Cl** (1832 cm^{-1}), and **5-Resf** (1827 cm^{-1}) all fall within the range typical for neutral $\{RuNO\}^6$ nitrosyl containing dicarboxamide tetradentate ligands.[17] All four reported complexes are diamagnetic (as expected for $\{Ru\text{-}NO\}^6$ nitrosyls) and display narrow-width peaks in their ^1H NMR spectra in $CDCl_3$ (Supporting Information, Figure S5−S8).

We have previously shown that variation in constituents on the ligand frame can modulate the electronic absorption spectrum of the resulting ruthenium nitrosyl.[17d] For example, a red shift of the λ_{max} of the absorption band from 395 nm (in the case of [$(Me_2bpb)Ru(NO)(Cl)$] (**1-Cl**)) to 455 nm (in the case of [$(Me_2bQb)Ru(NO)(Cl)$] (**2-Cl**)) is accomplished by extending conjugation of the pyridine moiety by replacement with a quinoline donor (Figure 7, top panel).[17d] In addition, substitution of the phenylenediamine ring of R_2bQb^{2-} type ligands with electron donating groups of increasing strength (Me < OMe) lowers the energy of the absorption band λ_{max} further to 490 nm (in the case of [$((OMe)_2bQb)Ru(NO)(Cl)$] (**3-Cl**)).[18b] Along the same line, **4-Cl** displays a red shift in λ_{max} (395 to 420 nm) because of the replacement of the Me substituents (in **1-Cl**) with OMe groups on the R_2bpb^{2-} ligand frame (Figure 7, top panel). Interestingly, the absorption band of **4-Cl** is more intense (ε = 7 800 M^{-1} cm^{-1}) than the corresponding absorption bands of **1-Cl** (ε = 5300 M^{-1} cm^{-1}),[17d] **2-Cl** (ε = 3 200 M^{-1} cm^{-1}),[17d] and **3-Cl** (ε = 3750 M^{-1} cm^{-1}).[18b]

The electronic absorption spectrum of **5-Cl** has an intense absorption band with λ_{max} of 475 nm (ε = 8700 M^{-1} cm^{-1}). Replacement of the quinoline moiety of **3-Cl** with 1-isoquinoline in **5-Cl**, results in a 15 nm blue shift in its λ_{max} value. However, there is an increase in the intensity of the absorption band of **5-Cl**. Clearly, elimination of the twist in the equatorial plane (Figure 5) accentuates the light-absorbing capacity of the nitrosyl in this set. Comparison of the intensities of the visible bands of **1-Cl** and **4-Cl** (both devoid of twist in the equatorial plane) indicates that replacement of Me with OMe groups on the phenylenediamine moiety of the ligand frame also improves the light harvesting capacity of the resulting nitrosyls.

To further enhance the sensitivity of **4-Cl** and **5-Cl** toward visible light, we have replaced the chloride ligands (trans to NO) with resorufin dye forming **4-Resf** and **5-Resf**. The absorption spectra of both Resf-conjugates contain additional intense absorption bands at 500 nm (ε = 29000 M^{-1} cm^{-1} and 31000 M^{-1} cm^{-1} respectively in $CHCl_3$). Interestingly, the deprotonated form of the unbound dye ($Resf^-$) has an intense absorption band at 590 nm (ε = 105000 M^{-1} cm^{-1} in DMF). Upon coordination to the positively charged metal center, a blue shift of the dye band (with concomitant reduction in extinction

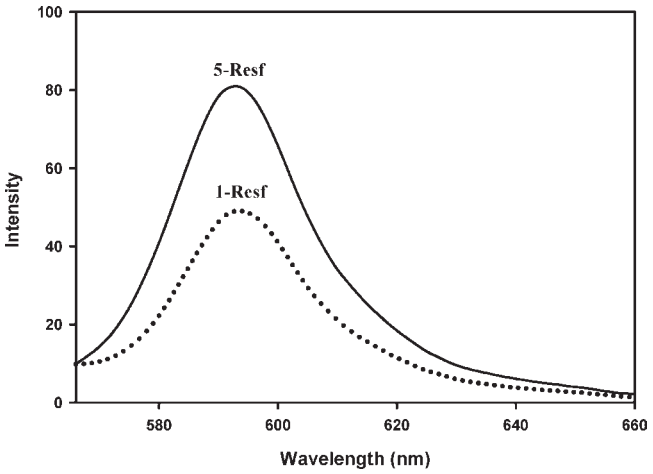

Figure 8. Fluorescence emission spectrum of **5-Resf** and **1-Resf** in MeCN (λ_{ex} = 490 nm). Samples with same absorbance values at 490 nm were used.

coefficient) occurs in the nitrosyl-dye conjugates. We have previously assigned such changes to the loss of delocalization of negative charge over the heterocyclic π-system and the loss of overall symmetry of the dye upon coordination. Indeed, simple protonation of $Resf^-$ also brings about similar changes in its electronic absorption spectrum (λ_{max} = 470 nm, ε = 20 000 M^{-1} cm^{-1} in DMF).[19]

A comparison of the five Ru-Resf complexes (**1-Resf** through **5-Resf**) reveals a uniform shift in the λ_{max} of the dye absorption band to 500 nm upon complexation. However, the ε-values of these complexes are greatly varied. For example, **1-Resf** and **2-Resf** both have ε-values around 12 000 M^{-1} cm^{-1}[18b] while **3-Resf**, **4-Resf**, and **5-Resf** have ε-values around 30 000 M^{-1} cm^{-1}. The most apparent difference between the two sets of complexes is the presence of Me versus OMe substituents on the tetradentate ligand frame. It therefore appears that in these nitrosyl-dye conjugates, the substituents on the ligand frame have more pronounced effect on the overall capacity of light absorption compared to the twist of the frame in the equatorial plane.

In addition to enhanced capacity of visible light absorption, the nitrosyl-dye conjugates also exhibit fluorescence arising from the bound dye moiety. Solutions of free resorufin in its deprotonated form are highly fluorescent. Upon direct coordination of the dye to the $\{RuNO\}^6$ center, the fluorescence is significantly quenched presumably because of energy transfer from the dye to the $\{RuNO\}^6$ unit. However, solutions of both **4-Resf** and **5-Resf** in MeCN still exhibit broad red fluorescence emission bands of moderate intensity at 593 nm (Figure 8). Similar fluorescence properties have previously been observed with **1-Resf**−**3-Resf**.[18b] In the case of **1-Resf**, the residual fluorescence was enough to monitor the location of complex during targeted NO delivery in a cellular environment.[18b] We anticipate similar use of these nitrosyl-dye conjugates as "trackable" NO donors in our future experiments.

NO Photolability. [((OMe)$_2$bpb)Ru(NO)(Cl)] (4-Cl) and [((OMe)$_2$IQ1)Ru(NO) (Cl)] (5-Cl). Exposure of solutions of the parent nitrosyls **4-Cl** and **5-Cl** in DMF to visible light promotes rapid release of NO (as evidenced by the responses of an NO-sensitive electrode). The photodissociation of NO is accompanied by the formation of a solvent bound Ru(III) photoproduct (eq 1), which typically exhibits a low-energy absorption band in its electronic spectrum. For example, photolysis of **4-Cl** in DMF under visible light (λ_{irr} > 465 nm) generates a low-energy absorption peak at 800 nm due to the Ru(III) photoproduct (Supporting Information, Figure S9). This transition has previously been assigned to a ligand-to-metal charge transfer (LMCT) from the negatively charged ligand (in this case $(OMe)_2bpb^{2-}$) to the Ru(III) center.[21] In addition, two other new absorption peaks at 270 and 375 nm along with clean isosbestic points at 280 and 325 nm are also generated following exposure of **4-Cl** to visible light. Under similar conditions, illumination of **5-Cl** also causes changes in its electronic absorption spectrum (Supporting Information, Figure S11). New broad absorption features at 425 and 640 nm are observed, and isosbestic points are noted at 310 and 335 nm.

$$(L)Ru\text{-}NO + h\nu + solv \rightarrow (L)Ru(III)\text{-}solv + NO^{\bullet} \quad (1)$$

Comparison of the quantum yield (ϕ) values of NO photorelease (in DMF) upon exposure to monochromatic 500 nm light of these chloride bound nitrosyls indicate that **5-Cl** (0.035 ± 0.005) is a more efficient NO donor than **4-Cl** (0.010 ± 0.005). Comparison of these values (Table 3) with those measured under similar conditions for **1-Cl**, **2-Cl**, and **3-Cl** reveals a trend in the efficiency of NO photorelease of **1-Cl** < **2-Cl** ~ **4-Cl** < **3-Cl** < **5-Cl**. This result confirms that alterations in the equatorial ligand frame do lead to increased sensitivity to visible light in ruthenium nitrosyls. In particular, removal of the twist in the equatorial ligand frame leads to increased NO photolability as exemplified by the trend **3-Cl** < **5-Cl**.

[((OMe)$_2$bpb)Ru(NO)(Resf)] (4-Resf) and [((OMe)$_2$-IQ1)Ru(NO)(Resf)] (5-Resf). A significant increase in the photosensitivity (to visible light) is noted with **4-Resf** and **5-Resf** in which the resorufin dye is directly coordinated to the Ru center. For instance, photolysis of **4-Resf** in MeCN under visible light (λ_{irr} > 465 nm) produces new absorption peaks at 390 and 650 nm in its absorption spectrum because of rapid photorelease of NO and concomitant formation of solvent bound Ru(III) photoproduct. (Supporting Information, Figure S10). Clean isosbestic points at 435 and 520 nm are also observed. In the case of **5-Resf**, illumination of a MeCN solution with visible light (λ_{irr} > 465 nm) causes the main dye-bound absorption band at 500 nm to blue shift incrementally to 470 nm and a new absorption feature at 675 nm to grow in (Figure 9). Clean isosbestic points at 330, 475, and 545 nm are also noted. Quantum yield (ϕ) values of these dye bound nitrosyls in DMF were measured to quantitatively compare the extent of photosensitization to visible light. Under illumination with monochromatic 500 nm light, **4-Resf** exhibits a ϕ_{500} value of 0.120 ± 0.008 which is much greater than that of the parent nitrosyls, **4-Cl**. The quantum yield of **5-Resf** (0.271 ± 0.008) is also higher than that of **5-Cl**, clearly showing the beneficial effect of direct dye conjugation. When all five resorufin bound

(21) (a) Bordini, J.; Hughes, D. L.; Da Motta Neto, J. D.; da Cunha, J. C. *Inorg. Chem.* **2002**, *41*, 5410–5416. (b) Sellmann, D.; Häuβinger, D.; Gottschalk-Gaudig, T.; Heinemann, F. W. *Z. Naturforsch.* **2000**, *55b*, 723–729.

Table 3. Summary of Absorption Parameters (λ_{max}, ε) and Quantum Yield (ϕ) Values of Selected Nitrosyls

complex	quantum yield ϕ (λ_{irr}, nm)	solvent	λ_{max}, nm (ε, M^{-1} cm^{-1})
[(Me bpb)Ru(NO)(Resf)] (**1-Resf**)[a]	0.052 ± 0.008 (500)	DMF	500 (11 920)
[(Me_2bQb)Ru(NO)(Resf)] (**2-Resf**)[a]	0.102 ± 0.009 (500)	DMF	500 (12 300)
[($(OMe)_2$bQb)Ru(NO)(Resf)] (**3-Resf**)[a]	0.206 ± 0.008 (500)	DMF	500 (27 100)
[(OMe_2bpb)Ru(NO)(Resf)] (**4-Resf**)	0.120 ± 0.008 (500)	DMF	500 (29 000)
[(OMe_2IQ1)Ru(NO)(Resf)] (**5-Resf**)	0.271 ± 0.008 (500)	DMF	500 (31 000)
[(Me_2bpb)Ru(NO)(Cl)](**1-Cl**)	0.0008 ± 0.0002 (500)	DMF	395 (5 300)
[(Me_2bQb)Ru(NO)(Cl)] (**2-Cl**)	0.010 ± 0.003 (500)	DMF	455 (3 200)
[($(OMe)_2$bQb)Ru(NO)(Cl)] (**3-Cl**)	0.025 ± 0.003 (500)	DMF	490 (3750)
[($(OMe)_2$bpb)Ru(NO)(Cl)](**4-Cl**)	0.010 ± 0.005 (500)	DMF	420 (7 800)
[($(OMe)_2$IQ1)Ru(NO)(Cl)] (**5-Cl**)	0.035 ± 0.005 (500)	DMF	475 (8 700)
[(Py_3P)Ru(NO)]BF_4[b]	0.050 ± 0.004 (532)	MeCN	530 sh (400)
[$Ru(NH_3)_5$(pz)Ru(bpy)$_2$(NO)]$(PF_6)_5$[c]	0.025 ± 0.002 (532)	H_2O	530 (9 550)
Roussin's Salt Ester (RSE)[d]	0.00019 ± 0.00005(546)	$CHCl_3$	364 (8 500)
PPIX-RSE[e]	0.00025 ± 0.00005(546)	$CHCl_3$	538 (10 200)
Fluor-RSE[f]	0.0036 ± 0.0005(436)	MeCN/H_2O	506 (72 200)

[a] Ref 18b. [b] Ref 17c. [c] Ref 22. [d] Ref 23. [e] Ref 24. [f] Ref 25.

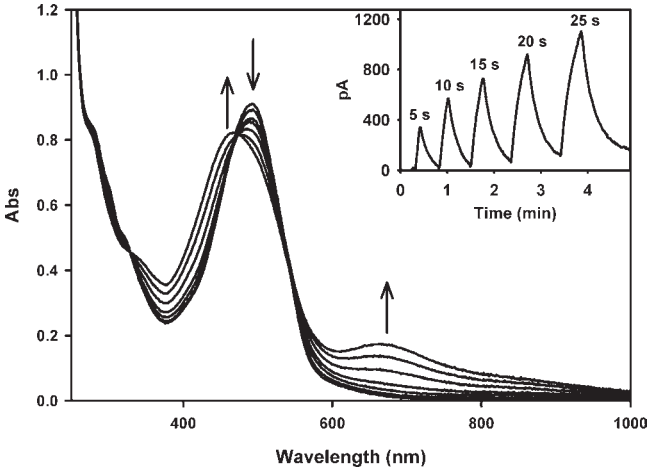

Figure 9. Changes in the electronic absorption spectrum upon photolysis of **5-Resf** in MeCN following illumination with visible light. Inset: NO amperogram of **5-Resf** in MeCN/H_2O upon illumination with visible light for time periods (in seconds) as indicated.

ruthenium nitrosyls are compared (**1-Resf** through **5-Resf**, Table 3), those with OMe-substituted ligand frames exhibit higher ϕ_{500} values than the Me-bearing ligands. Increased visible light absorption by the OMe-substituted complexes is presumably responsible for such enhancement. Removal of ligand twist enhances the ϕ_{500} value of **5-Resf** further to the maximum of 27%.

Summary and Conclusions

The following are the summary and conclusions of this investigation.

(a) Two new sets of chloride-bound (**4-Cl** and **5-Cl**) and Resf-bound (**4-Resf** and **5-Resf**) $\{RuNO\}^6$ nitrosyls have been synthesized from two designed tetradentate ligands that allowed assessment of the effects of ligand twists in the equatorial plane of these nitrosyls. The structures of **4-Resf**, **5-Cl** and **5-Resf** have been determined by X-ray crystallography.

(b) Unlike the previously reported **2-Cl**, **3-Cl**, **2-Resf**, and **3-Resf** nitrosyls derived from the R_2bQb^{2-} ligand frame that induces ligand twist in their equatorial plane, the equatorial ligand frames in the present nitrosyls are planar. Such relief in the steric strain increases the stability of the nitrosyls in strongly coordinating solvents including water.

(c) In addition to stability in aqueous solution, removal of ligand twist enhances the sensitivity of the nitrosyls to visible light. As measured by the extinction coefficients and quantum yield values at 500 nm (ϕ_{500}), addition of OMe substituents on the ligand frame and removal of steric interactions between the quinoline moieties of the ligand both improve the sensitivity of the nitrosyls toward visible light. Thus **5-Resf** exhibits the highest sensitivity to 500 nm light.

(d) Direct coordination of the Resf dye results in significant quenching of its fluorescence in these dye-tethered nitrosyls. The residual fluorescence of the Resf-bound nitrosyls however is sufficient for tracking these photoactive NO donors in cellular targets. For example, the fluorescence intensity of **5-Resf** (present study) is similar to that of **1-Resf** (Figure 8) which has already been used as trackable NO donor in cellular studies.[18b]

Acknowledgment. Support from a grant from the National Science Foundation (CHE-0957251) is gratefully acknowledged. N.F. was partially supported by a COR-SRG grant from UCSC. We thank Dr. David Rogow for help in the crystallographic measurements. The X-ray facility at UCSC is supported by a NSF Major Research Instrumentation (MRI) grant (CHE-0521569).

Supporting Information Available: FTIR spectra (Figure S1−S4) and ^1H NMR spectra (S5−S8) for **4-Cl**, **4-Resf**, **5-Cl** and **5-Resf**, X-ray crystallographic data (in CIF format) for complexes **4-Resf**, **5-Cl**, and **5-Resf**, and changes in the electronic absorption spectrum upon photolysis of **4-Cl**, **4-Resf**, **5-Cl** (Figure S9−S11). This material is available free of charge via the Internet at http://pubs.acs.org.

(22) Sauaia, M. G.; de Lima, R. G.; Tedesco, A. C.; da Silva, R. S. *J. Am. Chem. Soc.* **2003**, *125*, 14718–14719.
(23) Conrado, C.; Bourassa, J. L.; Egler, C.; Wecksler, S.; Ford, P. C. *Inorg. Chem.* **2003**, *42*, 2288–2293.
(24) Conrado, C. L.; Wecksler, S.; Egler, C.; Magde, D.; Ford, P. C. *Inorg. Chem.* **2004**, *43*, 5543–5549.
(25) Wecksler, S. R.; Hutchinson, J.; Ford, P. C. *Inorg. Chem.* **2006**, *45*, 1192–1200.